Volume 20, No 3 | International Journal of Radiation Research, July 2022

A Study on the correlation between brain functional and structural changes and altered cognitive function after radiotherapy for nasopharyngeal carcinoma

C-H. Qin, S-J. Qiu, H-Z. Wang, F-H. Duan, D-L. Wu, X. Leng*

Medical Imaging Center, The First Affiliated Hospital of Guangzhou University of Chinese Medicine, Guangzhou, Guangdong 510405, P.R. China

► ***Original article***

Corresponding author:
Xi Leng, Ph.D.,
E-mail: *lengxi1022@163.com*

Received: November 2021
Final revised: February 2022
Accepted: February 2022

Int. J. Radiat. Res., July 2022; 20(3): 627-633

DOI: 10.52547/ijrr.20.3.16

Keywords: *Radiation-induced brain injury, resting-state functional magnetic resonance, brain gray matter volume, cognitive function.*

ABSTRACT

***Background*:** To explore the changes of brain function and structure after radiotherapy (RT) for nasopharyngeal carcinoma (NPC), to investigate their correlation with altered cognitive function and to promote the recognition of radiation-induced brain injury (RBI). ***Materials and Methods*:** Resting-state functional MRI (rs-fMRI) and three dimensional (3D) T1-weighted imaging scans were conducted on 32 patients and 34 healthy subjects. Cognitive function was assessed in all subjects using multiple cognitive scales. Differences in regional homogeneity (ReHo) and brain gray matter (GM) volumes between groups were analyzed using the DPARSF package and VBM methods. ***Results*:** ReHo in Cerebelum_Crus2_L of the NPC patients was significantly higher than that in the controls, and was significantly correlated with memory, general cognitive function, and executive ability. The GM volumes in right fusiform gyrus (FFG.R), left temporal pole: middle temporal gyrus (TPOmid.L), left inferior temporal gyrus (ITG.L), Cerebelum_6_L, and left middle frontal gyrus (MFG.L) in the patients were significantly reduced compared with the controls, and were markedly correlated with multiple cognitive scale scores. ***Conclusion*:** Damage to brain after radiotherapy mostly involving the temporal lobe and cerebellum, manifested by a compensatory increase in ReHo and a decrease in GM volume, both of which were significantly correlated with multiple cognitive impairments. ReHo and brain GM volume can be considered as sensitive biomarkers to monitor RBI.

INTRODUCTION

Nasopharyngeal carcinoma (NPC) is one of the most common malignant tumor of the neck and head [1]. As the most common treatment of choice for NPC, radiotherapy (RT) may cause radiation-induced brain injury (RBI), a serious complication of central nervous system [2]. With the improvement of the overall survival rate of patients with NPC, increasing attention has been given to the improvement of RT complications, especially the research involving RT-related neurocognitive dysfunction [3]. Early brain microscopic changes have been found to predict late brain injury [4]. Therefore, obtaining early imaging markers of RBI and the correlation between imaging markers and different cognitive impairments are helpful for the early identification of RBI, which is of great significance for early intervention and possible prevention of irreversible brain damage and cognitive impairment [5].

To explore of the state of many neuropsychiatric disorders such as RBI, resting-state functional magnetic resonance imaging (rs-fMRI) is a commonly used method [6]. In rs-fMRI, regional homogeneity (ReHo) is an important approach that reflects local temporal synchronization of the regional blood oxygen level-dependent signals, which allows reliable analysis of interactions between brain regions [7] as well as brain regional properties that reliably reflect changes in cognitive function [8]. Changes in ReHo are important for predicting the prognosis of diseases [9, 10]. In addition to causing abnormalities in brain function, radiation can also damage brain structures. Most previous RBI studies have focused on changes in brain white matter structures, whereas fewer studies have examined brain gray matter (GM). Studies have shown that GM damage occurs in 29% to 100% of patients after RT [11-13], often manifesting as a reduction of the volume for the GM, and exploring changes in brain GM volume after RT is also important for monitoring RBI. Additionally, previous RBI studies have also found that abnormal GM volume after RT is significantly related to the impairment of cognitive function. Thus, it is believed that the reduction of brain GM volume can be used as an imaging marker of cognitive decline [14, 15].

Patients with NPC develop multiple cognitive deficits after RT. However, the Montreal cognitive

[DOI: 10.52547/ijrr.20.3.16]

assessment (MoCA) scale, which was widely used in the previous researches, has been proven that is not sensitive enough for several important cognitive functions for NPC patients after RT, such as executive functions [16]. Therefore, a more comprehensive cognitive scale is needed for the assessment of the cognitive functions of NPC patients after RT. Motivated to address the above problems, in the present study, rs-fMRI and high-resolution T1WI data were used to explore the changes in brain tissue that were normal on conventional MRI after RT for NPC, to identify sensitive diagnostic biomarkers for RBI and to further investigate the changes of cognitive function with the use of multiple scales for NPC patients after RT. To our knowledge, this study is the first to utilize multiple scales to comprehensively study the correlation between cognitive function and changes of brain function as well as brain structure in patients with NPC after RT. The novelty of this study is to reveal the pathological basis of cognitive decline in NPC patients after RT by analyzing the correlation between abnormalities in brain function and structure and multiple cognitive impairments. This study aims to provide a basis to reveal the RBI pathogenesis, to promote the early identification of RBI, and to provide new targets for the prevention, delay and treatment of RBI.

MATERIALS AND METHODS

Subjects

Thirty-two participants with pathologically confirmed NPC (24 males and 8 females, age 28-63, mean age 45.47 ± 10.66) and thirty-four normal controls (NCs) were collected for rs-fMRI and three dimensional (3D) -T1WI scans. The case group included patients after RT, and all patients received their first 3D confocal and intensity RT (total dose/ split dose/number of irradiations 66-74 Gy/1.8-2.0 Gy/30-35 times). Before MRI, the participants were confirmed that not have intracranial lesion. As shown in (table 1), no statistically significant difference was noted in gender, age, or education between the NPC patients and controls. The study was approved by the ethics committee of the first affiliated hospital of Guangzhou university of Chinese Medicine (Registration number: 2020116, date of registration: March 2021.) and conducted according to the principles of the Declaration of Helsinki and approved guidelines. All subjects have signed an informed consent prior to participation.

Neurocognitive tests

A series of neuropsychological tests were performed for all participants, including the MoCA - basic (MoCA-B), digital span test (DST, includes forward and backward) [17], trail making test (TMT; includes parts A and B) [18], auditory verbal learning test (AVLT) [19], digit symbol substitution test (DSST) [20].

Image acquisition

Via using a 3.0T scanner (SIGNA EXCITE; GE Healthcare, Chicago, IL, USA), all of the data were acquired. The imaging parameters were as follows: (1) 3D-T1WI: echo time (TE) = 1.5 ms, repetition time (TR)= 5.5 ms, field of view = 256 × 256 mm^2, acquisition matrix = 256×256, flip angle = 12°, sagittal slices = 166, voxel size = 1×1×1 mm^3 and no interslice gap; (2) rs-fMRI: TE=35 ms, TR=2100 ms, field of view=240×240 mm^2, acquisition matrix=64×64, flip angle=90°, layer thickness=3.8 mm, axial images=40, voxel size=3.75×3.75×3.8 mm^3, and layer spacing=0 mm.

Table 1. Demographics, clinical data, and cognitive assessment of NPC patients after RT and HCs.

	PT group (n=32)	HCs (n=34)	Statistics	*P*-value
Clinical characteristics				
Age (years)	45.47 ± 10.66	39.62 ± 13.00	t= 1.992	0.051
Sex (M/F)	24/8	22/12	χ^2=0.827	0.363
Education (years)	11.06 ± 3.85	11.65 ± 4.21	t= -0.588	0.559
Cognitive scores				
MoCA-B	25.19 ± 2.71	27.97 ± 1.49	t= -5.220	<0.0001*
DSST	45.91±16.70	55.91±16.55	t= -2.444	0.017*
DST forward	12.84 ± 3.25	14.50 ± 2.57	t= -2.301	0.025*
DST back-ward	8.31 ± 2.13	8.76 ± 1.26	t= 1.057	0.294
DST	4.53 ± 1.61	5.74 ± 1.71	t= -2.943	0.005*
TMT-A	41.89±14.92	34.29±12.21	t= 2.269	0.027*
TMT-B	37.60±13.57	30.19±14.70	t= 2.125	0.037*
AVLT (immediate)	21.03 ± 3.54	25.91 ± 4.59	t= -4.811	<0.0001*
AVLT (5min)	8.56 ± 1.74	9.71 ± 1.98	t= -2.487	0.015*
AVLT (20min)	8.19 ± 1.67	9.76 ± 2.05	t= -3.415	0.001*
AVLT (recognition)	11.16 ± 1.11	11.41 ± 1.26	t= -0.873	0.386

Data analysis

ReHo calculations were conducted by the use of the Data Processing Assistant for Resting-State fMRI (DPARSF)[21] from the MATLAB 2013b platform (MathWorks, Natick, MA,USA). Steps were as follows: (1) the DICOM format of raw images were converted to the NIFTI format; (2) slice timing and realignment: participants with head motion greater than 3° of any angular motion or greater than 3 mm were rejected; (3) the functional images were aligned to 3D T1WI anatomical images, and the aligned functional images were normalized to a 3 × 3 × 3 mm^3 Montreal Neurological Institute (MNI) 152 template; (4) linear detrending and temporal filtering were conducted at the 0.01~0.08 Hz to avoid high-frequency noise and low-frequency drift; (5) ReHo calculation was performed, and the resulting images were smoothed by a Gaussian kernel. The 3D-T1WI data were calculated using the VBM toolbox on the Statistical

[DOI: 10.52547/ijrr.20.3.16]

Parametric Mapping software (SPM8). It automatically calculates the volumes of grey matter, white matter and cerebrospinal fluid [22].

Statistical analysis

The SPSS 20.0 package was applied to calculate the differences in measures, such as age, education level, and cognitive scale scores, by two independent samples t-tests. For gender differences, chi-square test was utilized. For multiple comparisons of the differences in ReHo values and GM volume between groups, gender, age, as well as education were treated as covariates with false discovery rate (FDR) correction. Similarly, controlling for sex, age and education, ReHo values and cerebral GM volumes, which differed between groups in the post radiotherapy group of patients, were correlated with cognitive scales using partial correlation analysis. $P < 0.05$ was thought statistically significant.

RESULTS

ReHo

The ReHo of Cerebelum_Crus2_L was significantly greater than that of NCs in patients in the post-RT NPC patient (PT) group (figure 1), and ReHo in the PT group was significantly negatively correlated with DST, DST-BACKWARD, AVLT immediate recall, as well as MoCA-B scores. Furthermore, the ReHo was significantly positively correlated with TMT-A scores (figure 2).

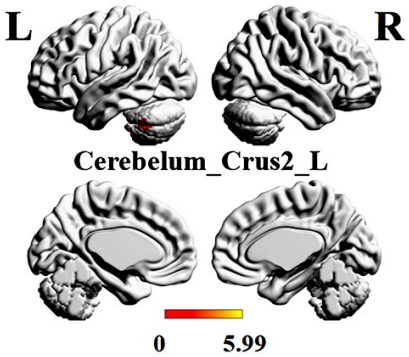

Figure 1. Brain regions with significant differences in ReHo between groups. ReHo in Cerebelum_Crus2_L of the patient group was significantly greater than that in normal controls (shown in red area).

Brain gray matter volume

The GM volumes of right fusiform gyrus (FFG.R), left temporal pole: middle temporal gyrus (TPOmid.L), left inferior temporal gyrus (ITG.L), Cerebelum_6_L, and left middle frontal gyrus (MFG.L) in the NPC PT were significantly reduced than NCs (figure 3). Among them, FFG.R GM volume was markedly positively correlated with DST-BACKWARD and MoCA-B scores. Furthermore, it was negatively correlated with TMT-A score. TPOmid.L GM volume was markedly positively correlated with MoCA-B, AVLT long-term delayed recall, and AVLT immediate recall scores. ITG.L GM volume was markedly positively correlated with MoCA-B and AVLT immediate recall scores. Cerebelum_6_L GM volume was significantly positively correlated with DST, DST-BACKWARD, AVLT immediate recall and MoCA-B scores. In addition, it was markedly negatively correlated with TMT-A scores. MFG.L GM volume was markedly positively correlated with DST-BACKWARD, AVLT immediate recall, and AVLT long-term delayed recall scores (figure 4).

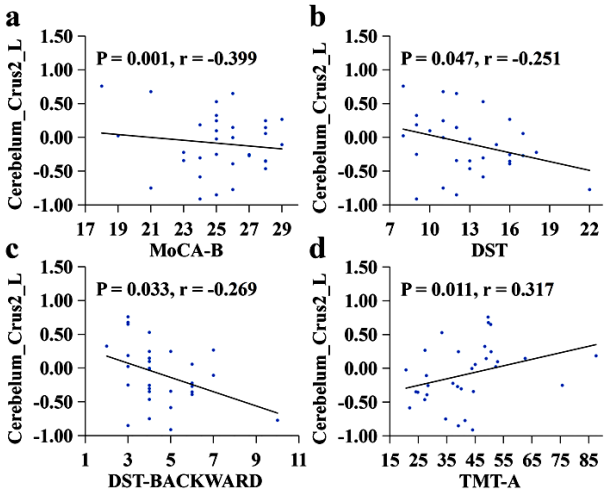

Figure 2. Correlation analysis of ReHo and cognitive function. ReHo in the patient group was significantly negatively correlated with MoCA-B **(a)**, DST **(b)**, and DST-BACKWARD **(c)** scores and significantly positively correlated with TMT-A scores **(d)**.

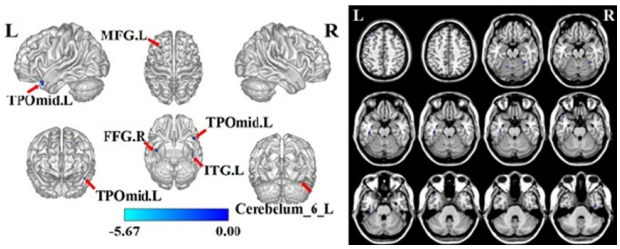

Figure 3. Brain regions with significant differences in GM volumes between groups. The brain GM volumes of FFG.R, TPOmid.L, ITG.L, Cerebelum_6_L, and MFG.L in the patient group were significantly reduced compared with those in normal controls [shown in blue area of the 3D brain map (the left side), and axial MRI images (the right side)]. FFG.R: right fusiform gyrus, TPOmid.L: left temporal pole: middle temporal gyrus, ITG.L: left inferior temporal gyrus, MFG.L: left middle frontal gyrus.

[DOI: 10.52547/ijrr.20.3.16]

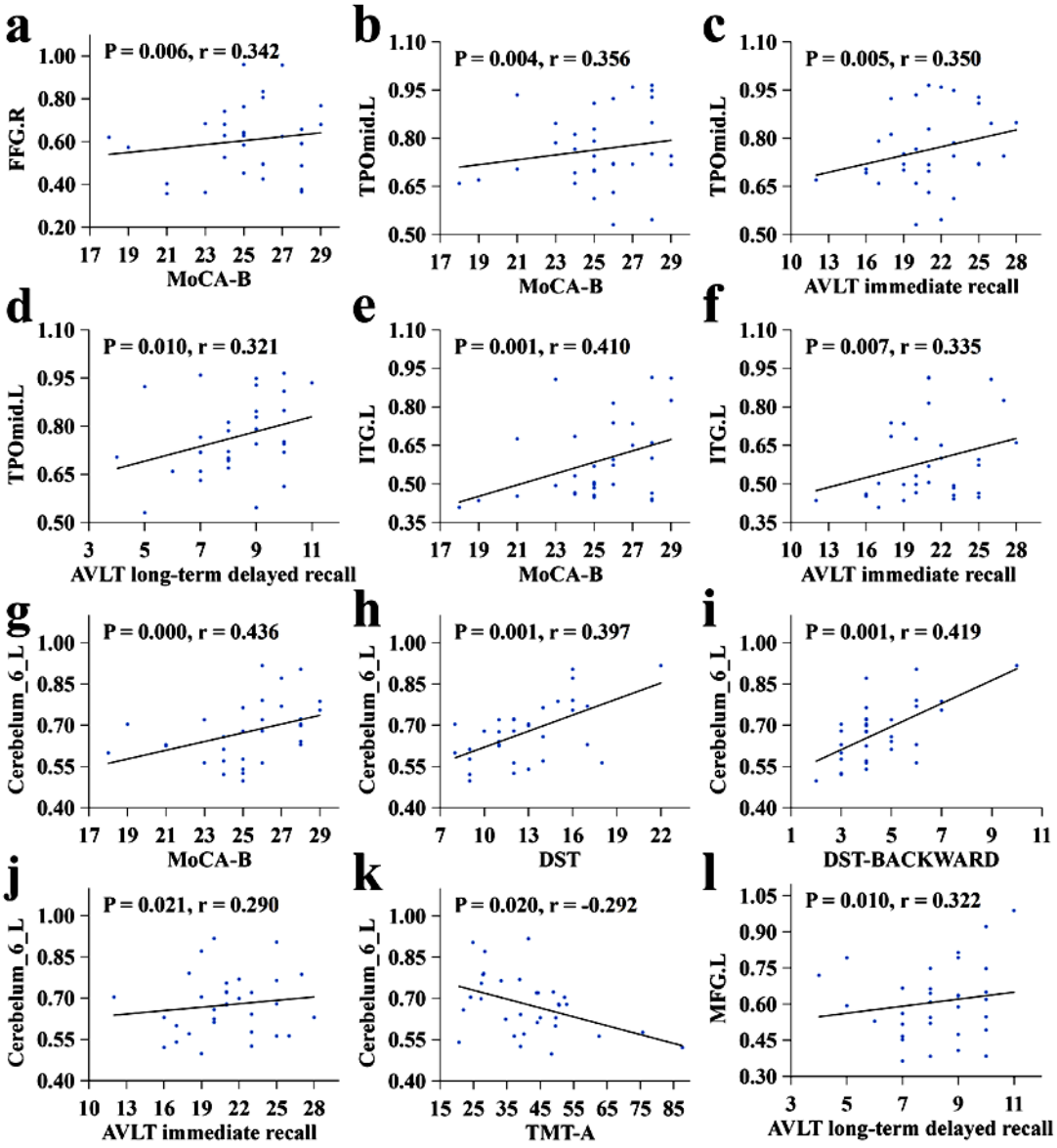

Figure 4. Correlation analysis of GM volumes and cognitive function. FFG.R GM volume was significantly positively correlated with MoCA-B scores **(a)**; TPOmid.L GM volume was significantly positively correlated with MoCA-B **(b)**, AVLT immediate recall **(c)**, and AVLT long-term delayed recall **(d)** scores; ITG.L GM volume was significantly positively correlated with MoCA-B **(e)** and AVLT immediate recall **(f)** scores; Cerebelum_6_L GM volume was significantly positively correlated with MoCA-B **(g)**, DST **(h)**, DST-BACKWARD **(i)**, and AVLT immediate recall **(j)** scores and significantly negatively correlated with TMT-A **(k)** scores; and MFG.L GM volume was significantly positively correlated with AVLT long-term delayed recall scores **(l)**.

DISCUSSION

We explored the difference of the brain function and GM structure in NPC patients with normal conventional head MRI performance after RT. For the first time, multiple cognitive scales were used to investigate the correlation between abnormalities in brain structure, brain function, and cognitive impairment. In studies of RBI [23, 24], the temporal lobe and cerebellum are often important targets of radiation injury, and these areas are close to or partially overlap with the radiation field of NPC in terms of anatomical location. If the radiation dose exceeds the brain tissue tolerance capacity, RBI is likely to occur. Brain regions with significantly abnormal brain function in this study were located in the cerebellum, and brain regions with markedly abnormal GM volumes were mainly in the cerebellum and temporal lobe. These findings are consistent with previous studies. Changes in cerebral blood flow can cause changes in blood oxygen level-dependent signals [25].

In our study, a markedly increase in ReHo in the cerebellum was observed, which may be related to increased cerebral blood flow due to RT, which is closely related to cerebrovascular injury. After irradiation, vasodilatation of brain tissue during the latency period, vascular endothelial cell injury, increased blood–brain barrier permeability, and increased vascularity are noted [26, 27], and these

[DOI: 10.52547/ijrr.20.3.16]

pathological changes may cause a promotion in blood flow to the injured region and an increase in ReHo. Hu *et al.* also found a significant promotion in blood flow to the left cerebellum in patients early after RT using arterial spin-labeled (ASL) MRI [28], which is consistent with the present study. This finding suggests that the brain tissue after RT may exhibit a transient elevation of blood flow due to local vascular injury, which causes abnormalities in regional brain functional signals, and the findings of the present study can give some evidence for the hypothesis of vascular injury in RBI. Some compensatory brain function often occurs after RT to maintain the general brain function, but the compensatory increase in function may also lead to late radiation brain necrosis [29].

We hypothesize that the ReHo value temporarily increases after RT due to vascular injury and the transient increase in local blood flow together with the compensatory effect of the brain functional network. This compensation phenomenon is not uncommon in other fMRI studies of RBI [6, 30, 31], and it maintains a certain information transmission efficiency of the brain network, thereby ensuring normal cognitive function. With the passage of time, damage to the blood–brain barrier gradually accumulates, and the compensation gradually diminishes. Thus, an increase in functional brain damage may consequently occur.

Yang *et al.* [5] found markedly differences in ReHo between patients with NPC after RT and controls and suggested that changes in brain functional activity as demonstrated by ReHo could allow early monitoring of RBI. However, the correlation between ReHo and cognitive scale scores was not analyzed in the study, and the mechanism of action between abnormal brain function and cognitive impairment is unclear. The present study used multiple scales to further investigate the correlation between ReHo and different cognitive functions, and several meaningful results were obtained. The ReHo of Cerebelum_Crus2_L was significantly negatively correlated with DST, DST-BACKWARD, AVLT immediate recall, and MoCA-B scores. Moreover, it was significantly positively correlated with TMT-A scores. Here, MoCA-B reflects general cognitive function, DST and AVLT reflect memory, and TMT reflects executive ability (the higher the TMT score, the worse the executive ability).

The results suggest that the local brain function of the left cerebellum becomes abnormal after RT. Although the ReHo is accordingly increased, it is significantly negatively correlated with general cognitive function, memory and executive ability, leading to multiple cognitive impairments. Previous research has demonstrated that the cerebellum might have an important role in cognition, and cerebellar damage was thought to be closely related to cognitive impairment [32]. In our study, the findings suggest that the brain function impairment mainly impairs general cognitive function, memory and executive ability. In a meta-analysis, it was observed that the patients with cerebellar lesions had significantly worse scores in neuropsychological tests, such as memory, semantic fluency and speech fluency [33], which was also reflected in our findings.

Another study found that lesions in the cerebellum lead to a cognitive-affective syndrome which was characterized by impaired executive function [34], which was also reflected in our findings, where we found that Reho in the cerebellum was negatively associated with executive ability.

In our study, the brain regions with markedly reduced GM volume included the temporal lobe, cerebellum, and frontal lobe, all of which have been shown to be radiation-prone brain regions in previous studies of RBI [5,35, 36]. In animal studies, glial cells in the brain GM were significantly damaged during the latency period of RBI with degeneration, apoptosis, and death of oligodendrocytes resulting in GM atrophy and hypofunction. Nagtegaal *et al.* [37] found a markedly reduction in brain GM thickness in several brain regions after RT in patients with glioma and concluded that this was significantly associated with cognitive impairment. Lv *et al.* [36] reported that GM volumes of the fusiform gyrus, precentral gyrus, as well as middle temporal gyrus were significantly reduced in patients after RT, and our study found similar results (such as fusiform gyrus, middle temporal gyrus).

In addition, hippocampal GM volume was significantly correlated with cognitive impairment [14], and the investigators concluded that brain GM volume can be sensitive for monitoring RBI. Guo *et al.* [15] found that a reduction in brain GM volume after RT was significantly related to cognitive impairment. Lin *et al.* [38] observed that GM thickness in the precentral gyrus was significantly reduced in patients after RT. Leng *et al.* [39] observed that the volume of brain GM was significantly reduced to varying degrees in NPC patients after RT, occurring in the bilateral frontal, temporal, parietal, cerebellar regions, and our study also found significant reductions in the GM volume in other regions in addition to the temporal lobe, such as the cerebellum and middle frontal gyrus. All of the above studies have shown that changes in brain GM volume after RT can be used as imaging markers of RBI.

However, the correlation between GM volume and different cognitive deficits remains unclear because the above studies either did not perform neuropsychological tests or only used the MoCA scale, which lacks a comprehensive assessment of multiple cognitive functions, and the association between different types of cognitive decline and GM volume reduction in NPC participants after RT was rarely discussed. In this study, RT was found to cause structural damage to GM in RBI-sensitive brain

[DOI: 10.52547/ijrr.20.3.16]

regions with a reduction in GM volume and leads to significant impairment of general cognitive function, memory, and executive ability. The temporal lobe and cerebellum are near to the radiation field of nasopharyngeal cancer radiotherapy, which are susceptible to radiation damage. In addition, temporal lobe belongs to default mode network (DMN), which is very sensitive to radiation [35].

Studies related to cognitive function have shown that impaired function within the DMN is associated with executive ability, attention, and memory [40]; in this study, similar results were observed. Cerebellum atrophy is related to cognitive impairment in a variety of neurological disorders. Just as cerebellar dysfunction can lead to cognitive impairment, cerebellar structural abnormalities can lead to decreased memory and executive function. The frontal lobe is an area in the DMN and the central executive network (CEN), which is closely related to the cognitive processes. Damage to the frontal lobe may cause cognitive deficits, especially executive function and working memory [41], which were also found in our findings.

Some limitations in our study should be noted. First, the sample size was small, and the sample size will be increased in the next step. Second, as a cross-sectional research, it cannot completely reveal the causal relationship between brain functional and structural changes in RBI and radiation, and a cohort study will be conducted in the next step. Third, all patients in this study received both chemotherapy and RT, and an effect of chemotherapy was possible. The next step should be to establish a separate RT group to eliminate this synergistic effect.

CONCLUSIONS

We demonstrated that damage to brain function and structure occurred after RT, mostly in the temporal lobe and cerebellum, as evidenced by a compensatory increase in ReHo and a decrease in GM volume, both of which were significantly associated with multiple cognitive impairments. This study provides evidence for revealing the pathogenesis of cognitive impairment after RT, and ReHo and GM volume can be used as sensitive markers for the monitoring of RBI.

ACKNOWLEDGEMENTS

The authors thank information specialist Wenli Dai from Peking University Third Hospital, Beijing, China, for assistance in the data analysis.

***Funding*:** This work was supported by the National Natural Science Foundation of China (grant numbers 81771344, 81920108019), the Natural Science Foundation of Guangdong Province (grant number 2018A030310621), and the Young Research Talent Training Program of The First Affiliated Hospital of Guangzhou University of Chinese Medicine (grant number 2017QN06).

***Ethical considerations*:** This study was approved by the ethics committee of The First Affiliated Hospital of Guangzhou University of Chinese Medicine. The registration number was 2020116, and the date was March 2021. The current study was carried out in accordance with the principles of the Declaration of Helsinki and the approved guidelines. All subjects signed informed consent before participating in the study.

***Conflict of interest*:** We declare that we have no conflict of interest.

***Author contribution*:** XL, CQ, and SQ contributed to conception and design of the study. XL, CQ, HW, FD, DW organized the data. XL and CQ performed the data analysis and drafted the manuscript. All authors revised the manuscript, and read and approved the submitted version.

REFERENCES

1. Xia C, Yu XQ, Zheng R, *et al.* (2017) Spatial and temporal patterns of nasopharyngeal carcinoma mortality in China, 1973-2005. *Cancer Lett*, ***401****: 33-38*.
2. Li Y, Huang X, Jiang J, *et al.* (2018) Clinical variables for prediction of the therapeutic effects of bevacizumab monotherapy in nasopharyngeal carcinoma patients with radiation-induced brain necrosis. *Int J Radiat Oncol Biol Phys*, ***100****: 621-629*.
3. Lin X, Tang L, Li M, *et al.* (2021) Irradiation-related longitudinal white matter atrophy underlies cognitive impairment in patients with nasopharyngeal carcinoma. *Brain Imaging Behav*, ***15****: 2426-2435*.
4. Makale MT, McDonald CR, Hattangadi-Gluth JA, *et al.* (2017) Mechanisms of radiotherapy-associated cognitive disability in patients with brain tumours. *Nat Rev Neurol*, ***13****: 52-64*.
5. Yang Y, Lin X, Li J, *et al.* (2019) Aberrant brain activity at early delay stage post-radiotherapy as a biomarker for predicting neurocognitive dysfunction late-delayed in patients with nasopharyngeal carcinoma. *Front Neurol*, **10**: 752.
6. Leng X, Qin C, Lin H, *et al.* (2021) Altered Topological Properties of Static/Dynamic Functional Networks and Cognitive Function After Radiotherapy for Nasopharyngeal Carcinoma Using Resting-State fMRI. *Front Neurosci*, ***15****: 690743*.
7. Zuo XN and Xing XX (2014) Test-retest reliabilities of resting-state FMRI measurements in human brain functional connectomics: a systems neuroscience perspective. *Neurosci Biobehav Rev*, ***45****: 100-118*.
8. Zhao Z, Tang C, Yin D, *et al.* (2018) Frequency-specific alterations of regional homogeneity in subcortical stroke patients with different outcomes in hand function. *Hum Brain Mapp*, ***39****: 4373-4384*.
9. Lin WC, Hsu TW, Chen CL et al (2015) Resting State-fMRI with ReHo Analysis as a Non-Invasive Modality for the Prognosis of Cirrhotic Patients with Overt Hepatic Encephalopathy. *PLoS One*, ***10****: e0126834*.
10. Nguyen KP, Raval V, Treacher A, *et al.* (2021) Predicting Parkinson's disease trajectory using clinical and neuroimaging baseline measures. *Parkinsonism Relat Disord*, ***85****: 44-51*.
11. Chan YL, Leung SF, King AD, *et al.* (1999) Late radiation injury to the temporal lobes: morphologic evaluation at MR imaging. *Radiology*, ***213****: 800-807*.
12. Chong VF, Fan YF, Mukherji SK (2000) Radiation-induced temporal lobe changes: CT and MR imaging characteristics. *AJR Am J Roentgenol*, ***175****: 431-436*.
13. Norris AM, Carrington BM, Slevin NJ (1997) Late radiation change in the CNS: MR imaging following gadolinium enhancement. *Clin Radiol*, ***52****: 356-362*.
14. Lv X, He H, Yang Y, *et al.* (2019) Radiation-induced hippocampal atrophy in patients with nasopharyngeal carcinoma early after

[DOI: 10.52547/ijrr.20.3.16]

radiotherapy: a longitudinal MR-based hippocampal subfield analysis. *Brain Imaging Behav*, ***13**: 1160-1171*.
15. Guo Z, Han L, Yang Y, *et al.* (2018) Longitudinal brain structural alterations in patients with nasopharyngeal carcinoma early after radiotherapy. *Neuroimage Clin*, ***19**: 252-259*.
16. Chapman CH, Nagesh V, Sundgren PC, *et al.* (2012) Diffusion tensor imaging of normal-appearing white matter as biomarker for radiation-induced late delayed cognitive decline. *Int J Radiat Oncol Biol Phys*, ***82**: 2033-2040*.
17. Diamond A (2013) Executive functions. *Annu Rev Psychol*, ***64**: 135-168*.
18. Muir RT, Lam B, Honjo K, *et al.* (2015) Trail making test elucidates neural substrates of specific poststroke executive dysfunctions. *Stroke*, ***46**: 2755-2761*.
19. Zhao Q, Guo Q, Liang X, *et al.* (2015) Auditory Verbal Learning Test is Superior to Rey-Osterrieth Complex Figure Memory for Predicting Mild Cognitive Impairment to Alzheimer's Disease. *Curr Alzheimer Res*, ***12**: 520-526*.
20. Chen X, Hu N, Wang Y, *et al.* (2020) Validation of a brain-computer interface version of the digit symbol substitution test in healthy subjects. *Comput Biol Med*, ***120**: 103729*.
21. Chao-Gan Y and Yu-Feng Z (2010) DPARSF: A MATLAB Toolbox for "Pipeline" Data Analysis of Resting-State fMRI. *Front Syst Neurosci*, ***4**: 13*.
22. Whitwell JL (2009) Voxel-based morphometry: an automated technique for assessing structural changes in the brain. *J Neurosci*, ***29**: 9661-9664*.
23. Qiu Y, Guo Z, Han L, *et al.* (2018) Network-level dysconnectivity in patients with nasopharyngeal carcinoma (NPC) early post-radiotherapy: longitudinal resting state fMRI study. *Brain Imaging Behav*, ***12**: 1279-1289*.
24. Gazdzinski LM, Cormier K, Lu FG, *et al.* (2012) Radiation-induced alterations in mouse brain development characterized by magnetic resonance imaging. *Int J Radiat Oncol Biol Phys*, ***84**: e631-638*.
25. Mulderink TA, Gitelman DR, Mesulam MM, *et al.* (2002) On the use of caffeine as a contrast booster for BOLD fMRI studies. *Neuroimage*, ***15**: 37-44*.
26. Diserbo M, Agin A, Lamproglou I, *et al.* (2002) Blood-brain barrier permeability after gamma whole-body irradiation: an *in-vivo* microdialysis study. *Can J Physiol Pharmacol*, ***80**: 670-678*.
27. Xu X, Huang H, Tu Y, *et al.* (2021) Celecoxib Alleviates Radiation-Induced Brain Injury in Rats by Maintaining the Integrity of Blood-Brain Barrier. *Dose Response*, ***19**: 15593258211024393*.
28. Hu F, Li T, Wang Z, *et al.* (2017) Use of 3D-ASL and VBM to analyze abnormal changes in brain perfusion and gray areas in nasopharyngeal carcinoma patients undergoing radiotherapy. *Biomed Res*, ***28**: 7879–85*.
29. Chen Q, Lv X, Zhang S, *et al.* (2020) Altered properties of brain white matter structural networks in patients with nasopharyngeal carcinoma after radiotherapy. *Brain Imaging Behav*, ***14**: 2745-2761*.
30. Wang HZ, Qiu SJ, Lv XF, *et al.* (2012) Diffusion tensor imaging and 1H-MRS study on radiation-induced brain injury after nasopharyngeal carcinoma radiotherapy. *Clin Radiol*, ***67**: 340-345*.
31. Xiong WF, Qiu SJ, Wang HZ, *et al.* (2013) 1H-MR spectroscopy and diffusion tensor imaging of normal-appearing temporal white matter in patients with nasopharyngeal carcinoma after irradiation: initial experience. *J Magn Reson Imaging*, ***37**: 101-108*.
32. Cao S, Nie J, Zhang J, *et al.* (2021) The Cerebellum Is Related to Cognitive Dysfunction in White Matter Hyperintensities. *Front Aging Neurosci*, ***13**: 670463*.
33. Ahmadian N, van Baarsen K, van Zandvoort M, *et al.* (2019) The Cerebellar Cognitive Affective Syndrome-a Meta-analysis. *Cerebellum*, ***18**: 941-950*.
34. Schmahmann JD (2019) The cerebellum and cognition. *Neurosci Lett*, 688:62-75
35. Ding Z, Zhang H, Lv XF *et al.* (2018) Radiation-induced brain structural and functional abnormalities in presymptomatic phase and outcome prediction. *Hum Brain Mapp*, ***39**: 407-427*.
36. Lv XF, Zheng XL, Zhang WD, *et al.* (2014) Radiation-induced changes in normal-appearing gray matter in patients with nasopharyngeal carcinoma: a magnetic resonance imaging voxel-based morphometry study. *Neuroradiology*, ***56**: 423-430*.
37. Nagtegaal SHJ, David S, Snijders TJ, *et al.* (2020) Effect of radiation therapy on cerebral cortical thickness in glioma patients: Treatment-induced thinning of the healthy cortex. *Neurooncol Adv 2: vdaa060*.
38. Lin J, Lv X, Niu M, *et al.* (2017) Radiation-induced abnormal cortical thickness in patients with nasopharyngeal carcinoma after radiotherapy. *Neuroimage Clin*, ***14**: 610-621*.
39. Leng X, Fang P, Lin H, *et al.* (2017) Structural MRI research in patients with nasopharyngeal carcinoma following radiotherapy: A DTI and VBM study. *Oncol Lett*, ***14**: 6091-6096*.
40. Sestieri C, Corbetta M, Romani GL, *et al.* (2011) Episodic memory retrieval, parietal cortex, and the default mode network: functional and topographic analyses. *J Neurosci*, ***31**: 4407-4420*.
41. Astle DE, Luckhoo H, Woolrich M, *et al.* (2015) The Neural Dynamics of Fronto-Parietal Networks in Childhood Revealed using Magnetoencephalography. *Cereb Cortex, **25**: 3868-3876*.

[DOI: 10.52547/ijrr.20.3.16]